A Multiphysics Approach to Fundamental Conjugate Drying by Forced Convection

M.V. De Bonis, and G. Ruocco*
DITEC, Università degli studi della Basilicata
*Corresponding author: Campus Macchia Romana, 85100 Potenza Italy, gianpaolo.ruocco@unibas.it

Abstract: Heat and mass transfer involved in drying is studied by using COMSOL 3.4. The effect of air temperature on the performance of the drying process applied to fresh food slices is scrutinized, but the main feature is that the model allows to disregard the most limiting parameters in such modeling, i.e. the average heat and mass transfer coefficients at the food/substrate interface. Such assumptions are limiting in the sense that they are referred to average transfer conditions and general geometries.
COMSOL flexible formulation is exploited by using a special drying kinetic for the substrate, and by including a treatment of the dependence of the properties upon the residual moisture content. The model is properly validated with the available experimental measurements, as the numerical solution is discussed by emphasizing on the conjugate nature of the drying process. Due to its flexibility and generality, the model can be used in common industrial driers' optimization, even in the assumption of a laminar flow field.

Keywords: Food Engineering, Conjugate Formulation, Transport Phenomena

1 Introduction

Drying is one of the most common methods of preserving food, involving a complex combination of transport phenomena such as the application of heat and the removal of moisture. Drying systems optimization is still sought nowadays and therefore full understanding of these phenomena can help to improve process parameters and hence product quality, emphasizing on the external and internal process parameters that influence drying behavior. The former include temperature, velocity and relative humidity of the drying medium (air), while the latter include density, permeability, sorption-desorption characteristics and physical substrate properties.
Starting from the seminal works by Luikov and Whitaker a vast number of contributions has been reported in the last decades on porous and multi-phase media drying by air convection [5]. But in the past few years the multi-dimensional (distributed, transient) analysis has gained importance, specially for lumped moist products, as a considerable computing power became more available, therefore many such studies could be conducted and finalized. Shapes and detailed configurations were explored through a variety of approach, though always appealing to empirical, average (i.e., independent on surface locations) relationships for interface transfer calculations.
These limitations affected many of the available works on drying modeling in the last decade, as reviewed in [3], where the interested Reader is referred to.
As drying is eminently a conjugate phenomenon (which means, the transfer of mass and heat is solved simultaneously in both solid and fluid phases, and are strongly coupled through evaporation and properties variation on moisture and temperature), an innovative approach is to solve a model in which the mass and energy interface fluxes vary seamlessly in space and time as the solution of the field variables. In this paper such an approach is carried out for a drying vegetable substrate. Residual water and temperature fields are computed locally within the substrate, when this interacts with a forced, laminar air flow. The later assumption allows to focus on the basic aspects of flow transport, focussing upon the vapor and liquid water production/depletion and transport, which is dealt with by an ad-hoc first-order irreversible kinetics. Such kinetics is included to solve for transient, two-dimensional flow, temperature and moisture

fields. Realistic transfer exchanges are inherently considered that vary with process time and surface location, eliminating the need for empirical heat and mass transfer (averaged) coefficients evaluation.

2 Problem formulation

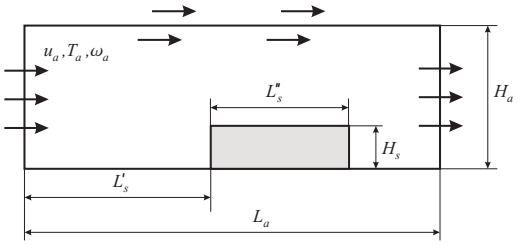

Figure 1: Geometry and nomenclature

Convection and moisture removal by a bulk, hot air draft is assumed to a model substrate, in this case carrot slices, as reported in Fig. 1. During processing, heat is transferred mainly by convection from air to the product's exposed surface, and by conduction from the surface toward the substrate interior. Meanwhile, moisture diffuses outward to the surface, where is vaporized. But if the substrate is water saturated, liquid can be converted into vapor even within the substrate, depending on the heat perturbation front. The water transport mechanisms generally include the motion of liquid water 1) by diffusion caused by differences in the concentration of solutes at the surface and in the interior (Fickian diffusion) and 2) by capillary forces, while the motion of water vapor is 3) by diffusion in air spaces within the substrate caused by vapor pressure gradients.

2.1 Assumptions

The following assumptions are considered in this work:

1. the flow is laminar; the dryer is two–dimensional, and a small portion in the vicinity of the product is studied only, for sake of simplicity;
2. due to the adopted flow regime, no body force is accounted for;
3. the thermophysical food properties are moisture–dependent, as reported by [3], while the air and water properties are temperature–dependent and are taken from [8]: for sake of simplicity their dependency are not reported in the formulation;
4. the effect of capillary forces is included in liquid water diffusivity;
5. the diffusivity of vapor in the substrate is the same than the diffusivity of liquid water, as implied for example by [4].

The following simplifying assumptions are adopted:

1. the viscous heat dissipation in the drying medium and the heat generation within the moist substrate are neglected;
2. due to the nature of the interacting species, no diffusion fluxes are accounted for in the energy equation;
3. neither shrinkage nor deformation of drying substrate are accounted for.

2.2 Governing equations

With reference to the previous assumptions, the governing conservation equations in vector form are enforced to yield for concentration of vapor and liquid water, pressure, velocity and temperature [2] in two distinct air and substrate sub–domains:

- In the substrate:
  Continuity, liquid water:
  $$\frac{\partial c_l}{\partial t} + \nabla \cdot (-D_{ls} \nabla c_l) = -K c_l \quad (1)$$
  Continuity, water vapor:
  $$\frac{\partial c_v}{\partial t} + \nabla \cdot (-D_{vs} \nabla c_v) = K c_l \quad (2)$$
  Energy:
  $$\rho_s c_{ps} \frac{\partial T}{\partial t} + \nabla \cdot (-k_s \nabla T) = -\dot{q}$$
- In the drying air:
  Continuity, water vapor:
  $$\frac{\partial c_v}{\partial t} + \nabla \cdot (-D_{va} \nabla c_v) = -\mathbf{u} \cdot \nabla c_v$$
  Momentum:
  $$\rho_a \left(\frac{\partial \mathbf{u}}{\partial t} + \mathbf{u} \cdot \nabla \mathbf{u} \right) = -\nabla p + \mu \nabla^2 \mathbf{u}$$
  Energy:
  $$\rho_a c_{pa} \frac{\partial T}{\partial t} + \nabla \cdot (-k_a \nabla T) = -\rho_a c_{pa} \mathbf{u} \cdot \nabla T$$

2.3 Evaporation cooling and vapor production rates

The cooling rate due to evaporation $\dot{q}$ can be computed as:

$$\dot{q} = \Delta h_{vap} M_l K c_l$$

The concept of rate of vapor production Kc is adopted in this paper: a negative source term Kc_l (K being the rate of production of water vapor mass per unit volume) is included in Eq. (1), to account for the depletion of liquid water; symmetrically, a positive source term Kc_v is included in Eq. (2), to account for the production of water vapor. The motivation of the kinetic–like approach for evaporation will be now briefly addressed. The first notion used to describe a drying process incorporating a single constant K for the combined effect of the various existing transport phenomena was suggested by W.K. Lewis in 1921, as recently recalled by [3] while reviewing the leading kinetic formulations. Since then, many variations of the basic equations have been reported in the open literature, based on purely empirical models, directly relating moisture ratio with drying time, and incorporating various parameters that describe both the inherent water phase conversion and interface conditions.
In this paper a modified exponential model of evaporation has been adopted, based on an Arrhenius first–order irreversible kinetics formulation. Several works have been presenting such an approach, as reviewed in the aforementioned work [3]. It is seen here that the inherent (volumetric) evaporation physics must be joined to interface conditions, such that the thermal, fluid dynamic and concentration regimes could be all be represented in the mass source term.
The present work is focussed upon the additional dependence on process temperature variation, so that the basic Arrhenius–type relationship can be modified as follows:

$$K = K_0 e^{-E_a/RT} K_1^{\alpha} \qquad (3)$$

where:

- K_0 is a reference constant, to be found empirically by matching a parametric numerical analysis with the available experimental/numerical data for each configuration, meaning that for a given configuration (air velocity/humidity, and geometry) K_0 is held constant in the present model;
- the activation energy E_a is taken as 48.7 kJ/mol;
- T is the local substrate temperature;
- K_1 is the ratio of the process temperature to the reference temperature;
- α is a dimensionless temperature factor varying with each different process temperature T_a.

It is emphasized here that present approach, that couples the heat and mass transfer through the use of the K and $\dot{q}$ source terms, simplifies the analysis with respect to the classical Luikov's approach, employed by [7] and [6].

2.4 Initial conditions

- For the substrate:
  initially in thermal equilibrium ($T = T_0$) with the quiescent ambient air the moisture content is such that:

  $$c_{l0} = 1000 \frac{U_0 \rho_s}{M_l}$$

  It is also $c_{v0} = 0$;
- for the drying air:
  with reference to Fig. 1, no–slip ($\mathbf{u} \equiv 0$) is enforced for the drying air at every solid surface; air flows, with a fully–developed (parabolic) horizontal component u_a, through the left inlet at given process temperature T_a and absolute humidity ω_a (as usual, related to the relative humidity) such that:

  $$c_{v0} = 1000 \frac{\omega_a \rho_a(T_a)}{(\omega_a + 1) M_l}$$

It is also $c_{l0} = 0$.

2.5 Boundary conditions

Full continuity is assumed for vapor mass and temperature through the substrate's surface, to solve for concentrations and temperature seamlessly across the interface. With reference to Fig. 1, the mass, momentum and thermal boundary conditions (where applicable) are as follows:

- Process inlet ($x = 0,\ 0 < y < H_a$):

$$c_v = c_{v0}\ , \quad u = u_a\ , \quad v = 0\ , \quad T = T_a$$

- Bottom plate, air interface ($0 < x < L'_s$ and $L'_s + L''_s < x < L_p\ ,\ y = 0$):

$$\frac{\partial c_{v,l}}{\partial y} = 0\ , \quad u = v = 0\ , \quad \frac{\partial T}{\partial y} = 0$$

- Bottom plate, substrate interface ($L'_s < x < L'_s + L''_s\ ,\ y = 0$):

$$\frac{\partial c_l}{\partial y} = 0\ , \quad \frac{\partial T}{\partial y} = 0$$

- Upper open surface ($0 < x < L_a\ ,\ y = H_p$):

$$\frac{\partial c_v}{\partial y} = 0\ , \quad \frac{\partial u}{\partial y} = \frac{\partial v}{\partial y} = 0\ , \quad \frac{\partial T}{\partial y} = 0$$

- Process outlet ($x = L_a\ ,\ 0 < y < H_a$):

$$\frac{\partial c_v}{\partial x} = 0\ , \quad \frac{\partial u}{\partial x} = 0\ , \quad v = 0\ , \quad \frac{\partial T}{\partial x} = 0$$

Finally, continuity is ensured by enforcing the following positions:

- Across the horizontal sub–domains interface ($L'_s < x < L'_s + L''_s\ ,\ y = H_s$):

$$c_{va} = c_{vs}\ , \quad \frac{\partial c_l}{\partial y} = 0,$$
$$u = v = 0\ , \quad T_a = T_s$$

- Across the upwind ($x = L'_s\ ,\ 0 < y < H_s$) and downwind ($x = L''_s\ ,\ 0 < y < H_s$) (vertical) sub–domains interfaces:

$$c_{va} = c_{vs}\ , \quad \frac{\partial c_l}{\partial x} = 0,$$
$$u = v = 0\ , \quad T_a = T_s$$

2.6 Numerical method and additional considerations

COMSOL 3.4 has been employed to integrate the partial differential equations system. Grid independency tests are not reported here for sake of brevity, and interested Readers are referred to the companion paper [3]. Execution time for $t = 18000$ s elapsed time has been approx. 20 min on a Pentium Xeon PC (WindowsXP Pro OS, 3.0 GHz, 2 GB RAM). Specific underrelaxation factors have been employed to solve the Navier–Stokes equations in the start–up phase of drying.

3 Results and discussion

3.1 Model validation

The available literature data are rather limited in order to validate the model and its numerical treatment, as geometry and flow regimes were always left unspecified and transfer coefficients were assumed from empirical correlations, except in [6] (who dealt with a non–food substrate). However, the experimental average residual moisture reported by [9] has been first compared with the present numerical solution and reported in Fig. 2. A 4–hrs baking process of a thin carrot slice with $L_s = 0.06$ m and $H_s = 0.0050$ or 0.0075 m (for Data Set 1 and 2, respectively) was configured with the following driving parameters: $T_a = 343$ or 323 K (for Data Set 1 and 2, respectively), $T_0 = 298$ K, $U_0 = 0.87$, and inlet air relative humidity of 45%. Care was exercised to adapt the present model so that the inlet air velocity u_a was 2.0 m/s, but still in the laminar regime, with $L_a = 0.20$ m and $H_a = 0.10$ m. The reference constant K_0 for the given configuration was 7×10^3, while the temperature factor α was found to be 0 and -10 for Data Set 1 and 2, respectively.
For Data Set 1 there is a good agreement at the beginning of treatment, while a maximum difference of approximately 15% is detected after 2 hrs. At the end of drying the measured and computed moisture are again very similar. In Data Set 2 the drying condition are milder therefore the kinetic parameters (in absence of a thickness adjustment) underestimate the measurements, the maximum difference being less than 10% after 3 hrs.
A second such benchmark has been found in the numerical data from [1] and reported in Fig. 3. A similar process (baking of a carrot substrate) was configured, with $L_s = 0.06$ m and $H_s = 0.015$, and with the following driving parameters: $T_a = 353$, 343 or 333 K (for Data Set 3 to 5, respectively), $T_0 = 303$ K, $U_0 = 0.64$, and inlet air relative humidity of 75%. Care was exercised, as well, to adapt the present model so that the inlet air velocity u_a was 0.3 m/s, in the laminar regime, with $L_a = 0.20$ m and $H_a = 0.10$ m. The reference constant K_0 for the given configuration was 90, while the temperature factor α was found to be 0, -17 and -10 for Data Set 3 to 5, respectively.

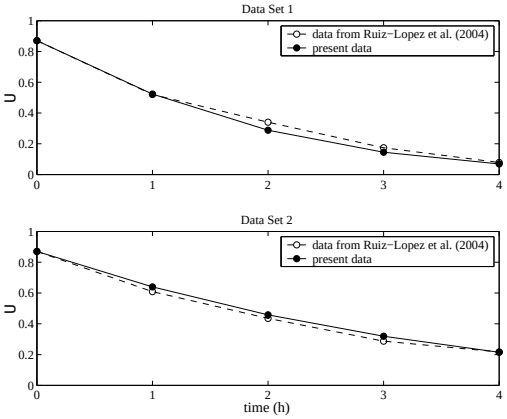

Figure 2: Average U evolution during process: comparison with [9] measurements for 2 different Data Sets

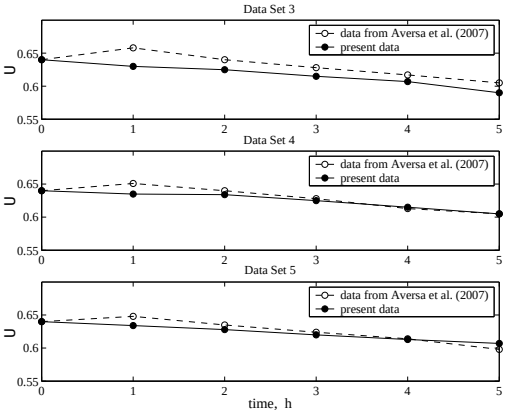

Figure 3: Average U evolution during process: comparison with [1] computations for 3 different Data Sets

The same limitations with the earlier benchmark were found, as no information was available on employed configuration. In all cases a good agreement is detected between the two different models. Small discrepancies (less than 5%) are found after 1 hr of treatment only, due to the condensation phenomenon reported in the benchmark work, which remains unjustified for empirical transfer coefficients such as the ones reportedly employed in [1].

3.2 Flow and temperature field

The simulation results for Data Sets 3 configuration [1] are then briefly presented in the form of velocity, temperature or moisture distributions. Figure 4 shows first the vector and scalar distributions of velocity in the drying air. Due to the flow field contraction and speed–up, the action of the drying air is strongest on top of the substrate, while the front and back faces are subject to stagnation and recirculation flow regions, respectively: this justifies the adoption of a fully conjugate model for a detailed description, as transfer properties vary considerably with exposed surface location.

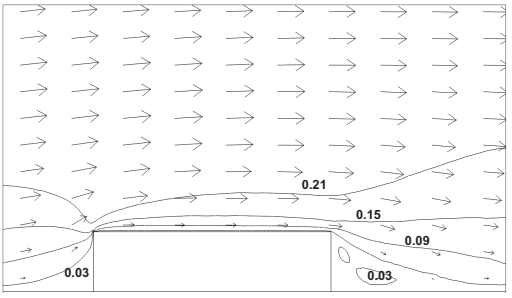

Figure 4: Close–up of flow field (vector field and streamlines) in the vicinity of substrate for Data Sets 3 to 5 fluid dynamic configuration, after a 5 hrs drying. $|\mathbf{u}|$ values range from 0 to 0.21 m/s

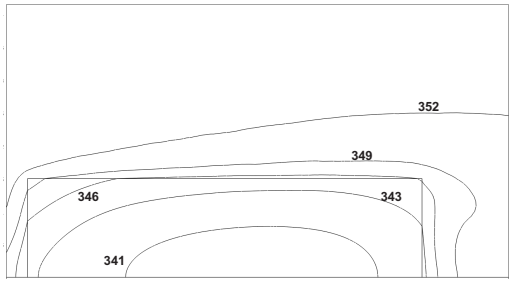

Figure 5: Close–up of temperature field (isotherms) in the substrate and its vicinity for Data Sets 3 configuration, after a 5 hrs drying. T values range from 341 to 352 K

Depending on the flow field, the temperature distribution in Fig. 5 presents a related non–homogeneous behavior, due to the non–uniform heat transfer, which will then reflect upon the residual moisture distribution. On the three exposed substrate sides, due to the conjugate nature of the model, the isotherms are obviously inclined. The substrate is found to be more than 3 K warmer on the leading edge, with respect to the trailing edge, and its left side is being heated more effectively (as expected) than the right one. The lowest temperature of about 340 K is detected on substrate bottom, by the adiabatic floor, with the slowest heating point being located slightly in the

flow direction.

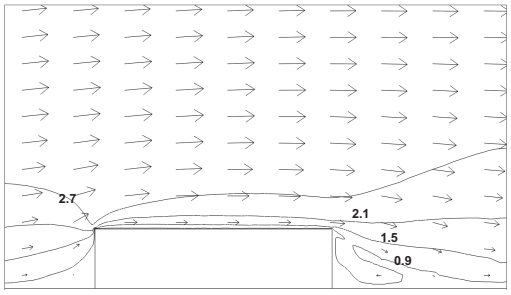

Figure 6: Close–up of flow field (vector field and streamlines) in the vicinity of substrate for a higher air velocity, after a 5 hrs drying. $|\mathbf{u}|$ values range from 0 to 2.7 m/s

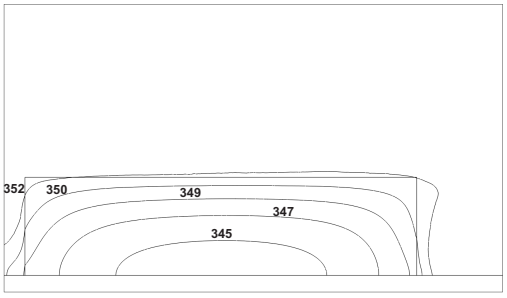

Figure 7: Close–up of temperature field (isotherms) in the substrate and its vicinity for a higher air velocity, after a 5 hrs drying. T values range from 345 to 352 K

In addition to the available Data Set 3, the present model has been exercised by varying the nominal value of velocity. Figure 6 shows the new flow field generated with $u_a = 0.3$ m/s, 10 times higher. The velocity distribution is very similar to the previous one, but the velocity local values are much higher indeed. These in turn reflect on the higher thermal regime, reported in Fig. 7, where the product center temperature increase by 4 K with respect to Data Set 3 comparison. A more dynamic flow situation dictates an overall more even side–to–side treatment, therefore the slowest heating point is almost perfectly centered this time.

3.3 Moisture and vapor removal

Based on the above flow field and temperature maps, it is expected that 1) the evaporation occurs non–homogeneously within the substrate, and 2) the vapor mass transfer across the fluid–substrate interface also occurs non–uniformly. Consequently, the moisture will be non–homogeneously removed within the substrate.

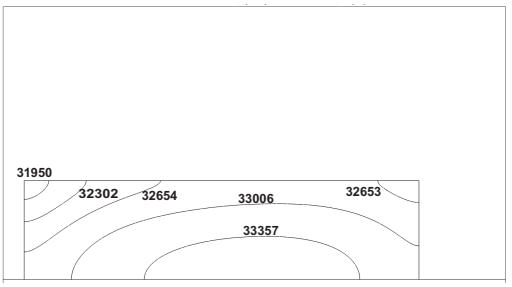

Figure 8: Close–up of residual moisture concentration field (isolines) in the substrate for Data Set 3 configuration, after a 5 hrs drying. c_l values range approximately from 3.19 to 3.33×10^4 mol/m^3

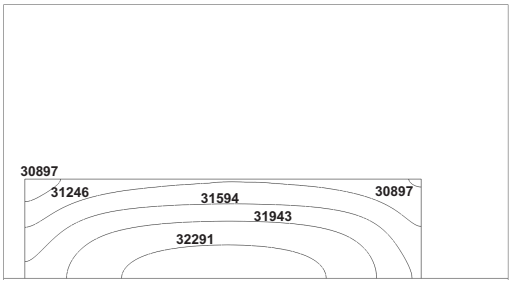

Figure 9: Close–up of residual moisture concentration field (isolines) in the substrate for a higher air velocity, after a 5 hrs drying. c_l values range approximately from 3.10 to 3.23×10^4 mol/m^3

Residual moisture distribution after the treatment is reported in Fig. 8 for Data Set 3. The evaporation and depletion of water is more effective where the temperature is the highest (Fig. 5) at the leading edge (a triangular chunk, one–fifth of the entire product), but the trailing edge is dried more than the average too, due to the favorable momentum transport in its vicinity.
Figure 9 describes the effect of ten–fold velocity increment on residual moisture. The drying process is stronger, so the humidity distribution decreases accordingly when compared with the Data Sets 3. The side–to–side treatment is slightly more homogeneous, but a larger concentration is detected y–wise in turn.

Conclusions

In this work a generalized conjugate model of forced convection drying has been worked out by using COMSOL 3.4. A modified exponential model for drying kinetics has been adopted, based on a modified Arrhenius first–order irreversible formulation, and validated against the available experimental or numerical literature data. Such an approach is independent on empirical heat and mass transfer coefficients.
The proposed model can be complemented by additional multi–physics effects such as microwave or ultrasound exposure, and can be readily extended to allow for full three–dimensional geometries by using COMSOL flexible features.

Nomenclature

α	temperature factor in Eq. (3) (-)
c	concentration (mol/m^3)
c_p	specific heat (J/kg K)
D	diffusivity (m^2/s)
Δh_{vap}	latent heat of evaporation (kJ/kg)
E_a	activation energy (kJ/mol)
k	thermal conductivity (W/mK)
K	rate of production (1/s)
K_0	reference constant (1/s) in Eq. (3)
K_1	temperature factor in Eq. (3) (-)
H	height (m)
L, L', L''	lengths (m)
M	molecular weight (g/mol)
μ	dynamic viscosity (Pa s)
ω	air absolute humidity (-)
p	pressure (Pa)
$\dot{q}$	evaporation cooling rate (W/m^3)
R	universal gas constant (kJ/mol K)
ρ	air density (kg/m^3)
t	time (s)
T	temperature (K)
u, v	components of air velocity (m/s)
$\mathbf{u}$	air velocity vector (m/s)
U	moisture content, wet basis (-)
x, y	coordinates (m)
X	moisture content, dry basis (-)

Subscripts

0	initial
a	air
l	liquid water
s	substrate, bulk
v	water vapor

References

[1] M. Aversa, S. Curcio, V. Calabrò, and G. Iorio, *An analysis of the transport phenomena occuring during food drying process*, Journal of Food Engineering **78** (2007), 922–932.

[2] R.B. Bird, W.B. Stewart, and E.N. Lightfoot, *Transport phenomena*, John Wiley & Sons, New York, 2002.

[3] M.V. De Bonis and G. Ruocco, *A generalized conjugate model for forced convection drying based on an evaporative kinetics*, Journal of Food Engineering **89** (2008), 232–240.

[4] L.M. Braud, R.G. Moreira, and M.B. Castell-Perez, *Mathematical modeling of impingement drying of corn tortillas*, Journal of Food Engineering **50** (2001), 121–128.

[5] P. Chen and D.C.T. Pei, *A mathematical model of drying processes*, International Journal of Heat and Mass Transfer **32** (1989), 297–310.

[6] K. Murugesan, H.N. Suresh, K.N. Seetharamu, P.A. Aswatha Narayana, and T. Sundararajan, *A theoretical model of brick drying as a conjugate problem*, International Journal of Heat and Mass Transfer **44** (2001), 4075–4086.

[7] L.S. Oliveira and K. Haghighi, *Mathematical modeling and numerical techniques*, ch. Finite element modeling of grain drying, pp. 309–338, Marcel Dekker, New York, 1997.

[8] R.H. Perry, D.W. Green, and J.O. Maloney, *Perry's chemical engineers' handbook*, McGraw-Hill, New York, 1997.

[9] I.I. Ruiz-López, A.V. Córdova, G.C. Rodríguez-Jimenes, and M.A. García-Alvarado, *Moisture and temperature evolution during food drying: effect of variable properties*, Journal of Food Engineering **63** (2004), 117–124.